Acta Crystallographica Section F
Structural Biology and Crystallization Communications
ISSN 1744-3091

Purification, crystallization and preliminary X-ray analysis of aminoglycoside-2″-phosphotransferase-Ic [APH(2″)-Ic] from *Enterococcus gallinarum*

Laura J. Byrnes,[a]‡ Adriana Badarau,[b] Sergei B. Vakulenko[b] and Clyde A. Smith[a]*

[a]Stanford Synchrotron Radiation Laboratory, Stanford University, Menlo Park, CA 94025, USA, and [b]Department of Chemistry and Biochemistry, University of Notre Dame, Notre Dame, IN 46556, USA

‡ Present address: Department of Biology, Rensselaer Polytechnic Institute, Troy, NY 12180, USA.

Correspondence e-mail: csmith@slac.stanford.edu

Received 26 November 2007
Accepted 14 January 2008

Bacterial resistance to aminoglycoside antibiotics is primarily the result of deactivation of the drugs. Three families of enzymes are responsible for this activity, with one such family being the aminoglycoside phosphotransferases (APHs). The gene encoding one of these enzymes, aminoglycoside-2″-phosphotransferase-Ic [APH(2″)-Ic] from *Enterococcus gallinarum*, has been cloned and the wild-type protein (comprising 308 amino-acid residues) and three mutants that showed elevated minimum inhibitory concentrations towards gentamicin (F108L, H258L and a double mutant F108L/H258L) were expressed in *Escherichia coli* and subsequently purified. All APH(2″)-Ic variants were crystallized in the presence of 14–20%(*w*/*v*) PEG 4000, 0.25 *M* $MgCl_2$, 0.1 *M* Tris–HCl pH 8.5 and 1 m*M* Mg_2GTP. The crystals belong to the monoclinic space group *C*2, with one molecule in the asymmetric unit. The approximate unit-cell parameters are a = 82.4, b = 54.2, c = 77.0 Å, β = 108.8°. X-ray diffraction data were collected to approximately 2.15 Å resolution from an F108L crystal at beamline BL9-2 at SSRL, Stanford, California, USA.

1. Introduction

A major factor in the emergence of antibiotic resistance is the existence of bacterial enzymes that chemically modify common antibiotics. One such family of antibacterials to which there is now almost universal resistance are the aminoglycosides. These broad-spectrum antibiotics were originally isolated from soil bacteria (Greenwood, 1995) and include a number of clinically relevant drugs such as tobramycin, kanamycin, gentamicin and amikacin. These molecules are targeted to the 30S ribosome and it has been proposed that aminoglycoside binding could lead to mistranslation of the mRNA owing to the binding of noncognate and near-cognate tRNAs (Vakulenko & Mobashery, 2003). However, there are now upwards of 80 bacterial enzymes (Davies & Wright, 1997; Smith & Baker, 2002) that chemically modify aminoglycosides. These enzymes are predominantly carried on mobile genetic elements, which facilitates their spread throughout bacterial populations, and fall into three classes: the coenzyme A-dependent acetyltransferases (AACs) and the ATP-dependent nucleotidyltransferases (ANTs) and phosphotransferases (APHs) (Smith & Baker, 2002; Vakulenko & Mobashery, 2003; Wright, 2003; Kim & Mobashery, 2005).

High-level resistance to gentamicin in enterococci is mediated by a group of four phosphotransferases. Optimal antibacterial therapy for enterococcal infections generally requires the use of ampicillin or vancomycin in conjunction with gentamicin and the synergistic effect resulting from this combination has proved to be critical for the treatment of serious infections. However, acquisition of gentamicin-specific phosphotransferases by enterococci has now eliminated this synergistic effect (Chow, 2000). The enzymes involved belong to the APH(2″) subfamily of aminoglycoside phosphotransferases, which preferentially phosphorylate at the 2″-hydroxyl group on the antibiotic. Structural details are known for one member of the subfamily, APH(2″)-Ib from *Enterococcus faecium* (Young *et al.*, 2008). Additional structural information is available for two other phosphotransferases from the APH(3′) subfamily: APH(3′)-IIa (Nurizzo *et al.*, 2003) and APH(3′)-III (Hon *et al.*, 1997; Burk *et al.*, 2001; Fong &

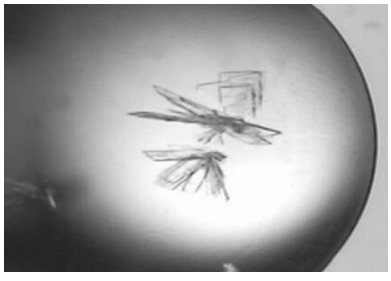

Berghuis, 2002). These enzymes phosphorylate at the 3′-hydroxyl of aminoglycosides including kanamycin, neomycin and butirosin. Gentamicin lacks a 3′-hydroxyl and is unaltered by the APH(3′) enzymes.

Structurally, the aminoglycoside phosphotransferase enzymes are all similar to each other and have a two-domain architecture which resembles the catalytic subunit of the eukaryotic Ser/Thr and Tyr protein kinases (Hon *et al.*, 1997; Nurizzo *et al.*, 2003). In APH(2″)-Ib the nucleotide-binding site is sandwiched between the N-terminal β-sheet domain and the C-terminal domain, with the gentamicin and streptomycin substrates bound in a negatively charged cleft in the C-terminal domain (Young *et al.*, 2008). Two highly conserved protein kinase fingerprint motifs (HGD*XXXX*N and ID*X*G) have been implicated in catalysis in the kinases and these motifs are present in the APH(2″) and APH(3′) phosphotransferase families. The conserved aspartate residue in the HGD*XXXX*N motif acts as the catalytic base (Zheng *et al.*, 1993) and is within hydrogen-bonding distance of the 2″-hydroxyl of gentamicin in APH(2″)-Ib (Young *et al.*, 2008).

As part of a program to define the molecular basis of aminoglycoside recognition and inactivation by the APH(2″) enzymes, we have cloned, purified and crystallized the APH(2″)-Ic enzyme from *E. gallinarum*. This enzyme differs somewhat from APH(2″)-Ib in that it shows a 100-fold selectivity for GTP over ATP (M. Toth, personal communication). Based upon sequence comparisons between the two enzymes, it is difficult to determine the cause of this nucleotide selectivity and efforts towards the determination of the molecular structure of APH(2″)-Ic are currently under way.

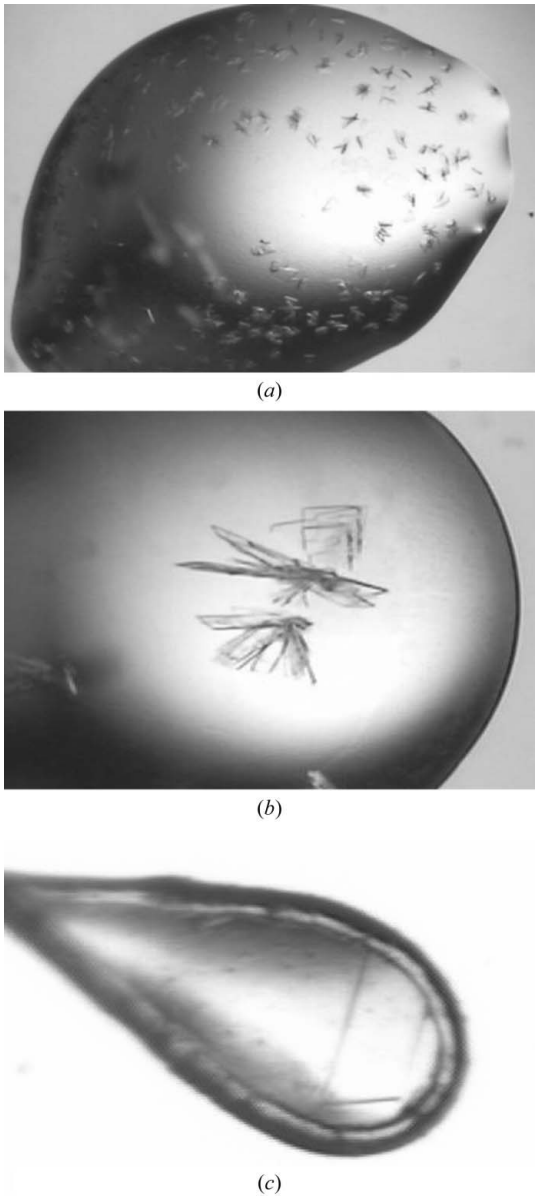

Figure 1
(*a*) Clusters of crystals of Mg_2GTP–APH(2″)-Ib F108L mutant obtained from the original Crystal Screen I condition No. 6. (*b*) Clusters of larger plates following fine screening. (*c*) The crystal used for data collection, with approximate dimensions of 0.20 × 0.1 × 0.01 mm.

2. Materials and methods

2.1. Cloning, expression and purification of APH(2″)-Ic wild-type and mutant enzymes

The wild-type *aph(2″)-Ic* gene and its mutant derivatives F108L, H258L and the double mutant F108L/H258L were recloned into the expression vector from the pBluescript II KS(+) vector (Kim *et al.*, 2004). The plasmid pBluescript::*aph(2″)-Ic* was digested with *Nde*I and *Hin*dIII and the *aph(2″)-Ic* gene and its mutants were cloned into the unique *Nde*I–*Hin*dIII sites of pET22a vector (Novagen). Chemically competent *Escherichia coli* BL21(DE3) cells were transformed with the resulting plasmids and selection was performed on LB agar supplemented with 100 µg ml^{-1} ampicillin. 1.4 l LB broth containing 100 µg ml^{-1} ampicillin and 25 m*M* L-proline was inoculated with 15 ml of an overnight culture of *E. coli* BL21(DE3) harboring the pET22a vector with cloned wild-type or mutant *aph(2″)-Ic* genes. The medium was incubated at 310 K in a shaking bath until the culture reached an optical density of 1.25 at 600 nm. The cultures were cooled to 283 K and IPTG was added to a final concentration of 0.8 m*M*. The cells were grown at 283 K (200 rev min^{-1}) for 16 h and were harvested by centrifugation at 3500*g*. The cell pellets were resuspended in 40 ml buffer *A* (25 m*M* HEPES pH 7.5, 0.2 m*M* DTT, 1 m*M* EDTA) and the bacteria were disrupted by sonication. The lysates were centrifuged at 21 000*g* for 30 min and streptomycin sulfate (1.5%) was added to the supernatant to precipitate nucleic acids. The resultant solutions were centrifuged at 3500*g* for 20 min followed by dialysis of the supernatant against two changes of buffer *A*. The dialysates were centrifuged at 3500*g* for 10 min and the supernatants were loaded onto kanamycin-affinity (Affi-Gel 15, BioRad) columns (2.5 × 10 cm) prepared as described previously (Kim *et al.*, 2004). The enzymes were eluted with a 25–40% linear gradient of buffer *B* (25 m*M* HEPES pH 7.5, 1 *M* NaCl, 0.2 m*M* DTT, 1 m*M* EDTA) in buffer *A* over two column volumes. Fractions were analyzed by a dibekacin phosphorylation assay and by SDS–PAGE for enzyme purity. Peak fractions were pooled, concentrated to 30 ml, dialyzed overnight against buffer *A* and applied onto gentamicin-affinity columns (2.5 × 10 cm) prepared as previously described (Kim *et al.*, 2004). APH(2″)-Ic and its mutants were eluted with a 55–75% gradient of buffer *B* in buffer *A* over two column volumes. Fractions of >95% purity were pooled, concentrated to 0.35 mg ml^{-1} and dialyzed against storage buffer (25 m*M* HEPES pH 7.5, 1 m*M* DTT). The wild-type APH(2″)-Ic and the three mutant derivatives were further concentrated either in storage buffer or in storage buffer supplemented with 1 m*M* Mg_2GTP to a final concentration of 6–10 mg ml^{-1}.

Table 1
Statistics of native data collection.

Values in parentheses are for the highest resolution shell.

Wavelength (Å)	0.9797
Space group	*C*2
Unit-cell parameters (Å, °)	a = 82.4, b = 54.2, c = 77.0, β = 108.8
Resolution range (Å)	50.0–2.15 (2.2–2.15)
Observed reflections	377107
Unique reflections	14484
Average redundancy	3.7
$R_{\rm merge}$† (%)	9.4 (45.5)
$\langle I/\sigma(I)\rangle$	6.4 (2.0)
Completeness (%)	97.1 (99.5)

† $R_{\rm merge} = \sum_{hkl}\sum_i |I_i(hkl) - \langle I(hkl)\rangle| / \sum_{hkl}\sum_i I_i(hkl)$, where $I_i(hkl)$ is the observed intensity of a given reflection and $\langle I(hkl)\rangle$ is the mean intensity for all observations of that reflection.

2.2. Crystallization

For all of the APH(2″)-Ic variants, initial coarse screens were performed with commercially available sparse-matrix screens (Crystal Screens I and II, Hampton Research) using the sitting-drop method. One condition from Crystal Screen I (condition No. 6; 30% PEG 4000, 0.2 *M* $MgCl_2$ 0.1 *M* and Tris HCl pH 8.5) resulted in spiky clusters of crystals (Fig. 1*a*) for the wild-type, F108L, H258L and the double mutant F108L/H258L proteins, all with Mg_2GTP. Further fine-screening experiments using the hanging-drop method resulted in crystals of the F108L mutant that were suitable for X-ray diffraction. The crystals grew as clusters of thin plates (Fig. 1*b*) in 2 µl drops containing protein at a concentration of 8.8 mg ml^{-1} in 25 m*M* HEPES buffer pH 7.5, 1 m*M* DTT and 1 m*M* Mg_2GTP. The crystallization drops contained a 1:1 mixture of protein and reservoir solutions; the reservoir solution consisted of 14–20% PEG 4000, 0.25 *M* $MgCl_2$ and 0.1 *M* Tris–HCl pH 8.5. The crystals grew at both 288 and 295 K and took about 3 d to reach maximum size (approximately 0.2 × 0.1 × 0.01 mm). The F108L crystal used for data collection is shown in Fig. 1(*c*).

2.3. Data collection and preliminary X-ray analysis

The Mg_2GTP–APH(2″)-Ic F108L crystals were harvested from the crystallization drop, flash-frozen immediately in liquid nitrogen with no additional cryoprotection and stored in a sample cassette designed for use with the Stanford Automated Mounting (SAM) system (Cohen *et al.*, 2002). The crystals were transferred to beamline BL9-1 at the Stanford Synchrotron Radiation Laboratory (SSRL) and screened for diffraction quality. X-ray diffraction data were collected on beamline BL11-1 from a single F108L crystal maintained at 100 K with an Oxford Cryosystem using a MAR Mosaic 325 CCD detector. A total of 180 images were collected with an oscillation range of 1° per image, an exposure time of 30 s and a crystal-to-detector distance of 400 mm. The data were processed with the program *MOSFLM* (Leslie, 1992) and scaled with *SCALA* from the *CCP*4 program suite (Collaborative Computational Project, Number 4, 1994). Table 1 gives a summary of the data-collection statistics.

Molecular replacement was attempted using the programs *MOLREP* (Vagin & Teplyakov, 1997) and *Phaser* (McCoy *et al.*, 2005), utilizing the structure of APH(2″)-Ib (Young *et al.*, 2008) as a search model.

3. Results and discussion

3.1. Crystallization

For each of the four APH(2″)-Ic variants (the wild type and the three mutants), the protein was prepared either as the apo form or as the Mg_2GTP complex. This proved to be very beneficial in that only the Mg_2GTP–APH(2″)-Ic complexes produced crystals under the PEG 3350 conditions. Initial fine screening of these crystallization conditions was attempted for all four Mg_2GTP–APH(2″)-Ic variants and in the initial experiments improvements in crystal form and habit were only observed for the F108L mutant. Additional fine screening of the conditions for this mutant yielded the clusters of thin plates shown in Fig. 1(*b*), which proved to be of sufficient quality for the collection of diffraction data. A complete data set was collected for the Mg_2GTP complex of the F108L mutant. The crystal diffracted to approximately 2.15 Å resolution (Fig. 2) and belonged to space group *C*2, with unit-cell parameters a = 82.4, b = 54.2, c = 77.0 Å, β = 108.8°. Calculation of the Matthews coefficient ($V_{\rm M}$; Matthews, 1968) using

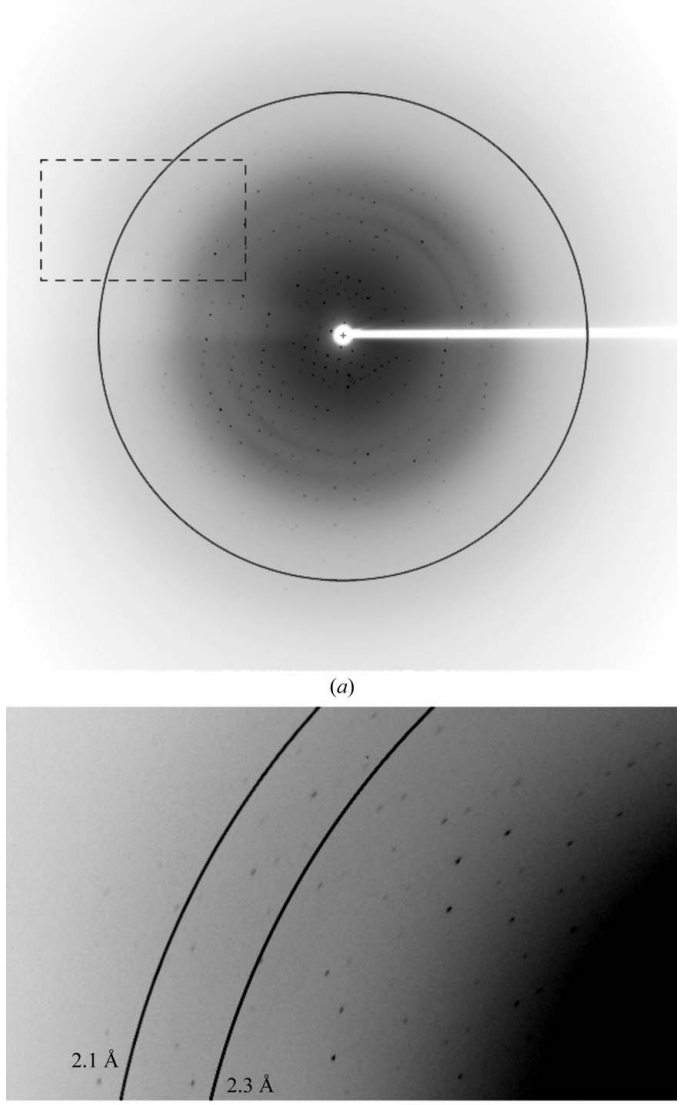

(*a*)

(*b*)

Figure 2
(*a*) Diffraction image of the Mg_2GTP–APH(2″)-Ic F108L mutant. The 2.3 Å resolution ring is indicated. (*b*) Close-up of the part of the image indicated by the dashed rectangle in (*a*).

an estimated molecular weight of 35 kDa gave a value of 2.3 Å^3 Da^{-1} (47% solvent content) assuming the presence of one molecule per asymmetric unit. Subsequent fine screening using the Mg_2GTP complex of the wild-type protein produced similar crystals (clusters of flat plates) under similar conditions (23–25% PEG 4000, 0.2 *M* $MgCl_2$, 0.1 *M* Tris–HCl pH 8.5 at 295 K).

Inspection of the original sparse-matrix screens showed that a second condition from Crystal Screen II (condition No. 36; 0.1 *M* HEPES pH 7.5, 4.3 *M* NaCl) gave spherical crystalline clusters for all four enzyme variants, irrespective of whether or not Mg_2GTP was present. One of these clusters was mounted in a loop, flash-frozen in liquid nitrogen and screened for diffraction on SSRL beamline BL9-1. The subsequent images clearly showed protein diffraction, albeit from multiple lattices. Additional screening around these conditions with the apo form of the APH(2″)-Ic F108L mutant produced clusters of small plate-like crystals and preliminary X-ray diffraction analysis showed that they diffracted to approximately 2.8 Å resolution and belonged to space group *P*2 or $P2_1$, with unit-cell parameters $a = 61.5$, $b = 86.6$, $c = 93.8$ Å, $\beta = 95.7^\circ$. Owing to the small size of these crystals and their rapid decay in the synchrotron beam, diffraction data have not yet been collected. Fine screening of these conditions is ongoing.

3.2. Molecular replacement

Although the level of amino-acid sequence identity between the members of the APH(2″) subfamily is somewhat low (25–31%), it was thought that molecular replacement using APH(2″)-Ib as a search model might provide reasonable starting phases for the APH(2″)-Ic structure. The APH(2″)-Ib model was modified using the program *CHAINSAW* from the *CCP*4 suite (Collaborative Computational Project, Number 4, 1994), replacing the nonconserved residues with alanine. Several different models were produced from this truncated model including separate domains and loop truncations, along with a polyalanine model. Although a weak solution which seemed to be consistent could be found from most input models with *MOLREP*, refinement of the model has so far proved unsuccessful. The solution using a polyalanine model derived from the *CHAINSAW*-truncated model gave the best results (*R* factor 0.53, score 0.197) and the phases from this solution were used to calculate a prime-and-switch density-modified composite OMIT map using the program *RESOLVE* (Terwilliger, 2000). Around 190 residues were subsequently built by *RESOLVE* and although this model refined somewhat better than the original model from *MOLREP*, the $R_{\rm free}$ remains high. In an attempt to obtain experimental phases, derivatization with krypton (Cohen *et al.*, 2001) and soaking experiments with a Gd-HPDO3A complex (Girard *et al.*, 2003) are being carried out. In addition, selenomethionine-substituted APH(2″)-Ib has been expressed and purified and crystallization trials are under way.

This work was supported by Grant No. AI057393 from the National Institutes of Health (SBV) and by Grant No. 5 P41 RR001209 from the National Center for Research Resources (SSRL). LJB was supported by a Summer Undergraduate Laboratory Internship. Portions of this research were carried out at the Stanford Synchrotron Radiation Laboratory, a national user facility operated by Stanford University on behalf of the US Department of Energy, Office of Basic Energy Sciences. The SSRL Structural Molecular Biology Program is supported by the Department of Energy (BES, BER) and by the National Institutes of Health (NCRR, BTP, NIGMS). The contents of this paper are solely the responsibility of the authors and do not necessarily represent the official view of NCRR or NIH.

References

Burk, D. L., Hon, W. C., Leung, A. K. & Berghuis, A. M. (2001). *Biochemistry*, **40**, 8756–8764.
Chow, J. W. (2000). *Clin. Infect. Dis.* **31**, 586–589.
Cohen, A., Ellis, P., Kresge, N. & Soltis, S. M. (2001). *Acta Cryst.* D**57**, 233–238.
Cohen, A. E., Ellis, P. J., Miller, M. D., Deacon, A. M. & Phizackerley, R. P. (2002). *J. Appl. Cryst.* **35**, 720–726.
Collaborative Computational Project, Number 4 (1994). *Acta Cryst.* D**50**, 760–763.
Davies, J. & Wright, G. D. (1997). *Trends Microbiol.* **5**, 234–240.
Fong, D. & Berghuis, A. M. (2002). *EMBO J.* **21**, 2323–2331.
Girard, É., Stelter, M., Vicat, J. & Kahn, R. (2003). *Acta Cryst.* D**59**, 1914–1922.
Greenwood, D. (1995). Editor. *Antimicrobial Chemotherapy*, pp. 32–48. Oxford University Press.
Hon, W. C., McKay, G. A., Thompson, P. R., Sweet, R. M., Yang, D. S. C., Wright, G. D. & Berghuis, A. M. (1997). *Cell*, **89**, 887–895.
Kim, C., Haddad, J., Vakulenko, S. B., Meroueh, S. O., Wu, Y., Yan, H. & Mobashery, S. (2004). *Biochemistry*, **43**, 2373–2383.
Kim, C. & Mobashery, S. (2005). *Bioorg. Chem.* **33**, 149–158.
Leslie, A. G. W. (1992). *Jnt CCP4/ESF–EACBM Newsl. Protein Crystallogr.* **26**.
McCoy, A. J., Grosse-Kunstleve, R. W., Storoni, L. C. & Read, R. J. (2005). *Acta Cryst.* D**61**, 458–464.
Matthews, B. W. (1968). *J. Mol. Biol.* **33**, 491–497.
Nurizzo, D., Shewry, S. C., Perlin, M. H., Brown, S. A., Dholakia, J. N., Fuchs, R. L., Deva, T., Baker, E. N. & Smith, C. A. (2003). *J. Mol. Biol.* **327**, 491–506.
Smith, C. A. & Baker, E. N. (2002). *Curr. Drug Targets Infect. Dis.* **2**, 143–160.
Terwilliger, T. C. (2000). *Acta Cryst.* D**56**, 965–972.
Vagin, A. & Teplyakov, A. (1997). *J. Appl. Cryst.* **30**, 1022–1025.
Vakulenko, S. B. & Mobashery, S. (2003). *Clin. Microbiol. Rev.* **16**, 430–450.
Wright, G. D. (2003). *Curr. Opin. Chem. Biol.* **7**, 563–569.
Young, P. G., Walanj, R., Lakshmi, V., Byrnes, L. J., Baker, E. N., Vakulenko, S. & Smith, C. A. (2008). In the press.
Zheng, J., Knighton, D. R., Ten Eyck, L. F., Karlsson, R., Xuong, N.-H., Taylor, S. S. & Sowadski, J. M. (1993). *Biochemistry*, **32**, 2154–2161.